

## Research Article

# A Novel Sensor for Noninvasive Detection of In Situ Stem Water Content Based on Standing Wave Ratio

Chao Gao,<sup>1,2,3</sup> Yue Zhao,<sup>1,2,3</sup> and Yandong Zhao <sup>1,2,3</sup>

<sup>1</sup>School of Technology, Beijing Forestry University, Beijing 100083, China

<sup>2</sup>Beijing Laboratory of Urban and Rural Ecological Environment, Beijing Municipal Education Commission, Beijing 100083, China

<sup>3</sup>Key Lab of State Forestry Administration for Forestry Equipment and Automation, Beijing 100083, China

Correspondence should be addressed to Yandong Zhao; [yandongzh@bjfu.edu.cn](mailto:yandongzh@bjfu.edu.cn)

Received 20 November 2018; Revised 8 January 2019; Accepted 16 January 2019; Published 27 March 2019

Academic Editor: Egidio De Benedetto

Copyright © 2019 Chao Gao et al. This is an open access article distributed under the Creative Commons Attribution License, which permits unrestricted use, distribution, and reproduction in any medium, provided the original work is properly cited.

Stem water content (StWC = volume of water : volume of stem) is an important physiological parameter for vascular plants. And a better understanding of StWC contributes to solving some research hotspots in forestry, such as drought resistance, cold resistance, precise irrigation, and health assessment. However, there are few noninvasive, in situ, real-time, safe, and low-cost methods for detecting StWC of woody plants. This article presents a novel sensor for noninvasive detection of in situ StWC based on standing wave ratio. Moreover, extensive experiments were conducted to analyze the performance of this sensor including sensitive distance, measuring range, influence factors, and measuring accuracy. The experimental results show that the sensitive distance of StWC sensor is approximately 53 mm in axial direction and 20 mm in radial direction with the measuring range from 0.01 to 1.00 cm<sup>3</sup> cm<sup>-3</sup>. The combined effects of stem EC and temperature on sensor output are significant and it is necessary to correct the error caused by the two factors. Compared with the oven-drying method, StWC sensor has higher measuring accuracy than Testo 606-2 which is a sensor for measuring wood water content and its average error is less than 0.01 cm<sup>3</sup> cm<sup>-3</sup>. In addition, StWC sensor performed very well on the crape myrtle with high sensitivity equal to 1022.1 mV (cm<sup>3</sup> cm<sup>-3</sup>)<sup>-1</sup> and measuring results also accorded with the diurnal dynamics of stem water content.

## 1. Introduction

A stem is one of the two main structural axes of the vascular plant and plays multiple roles in the plant, such as the mechanical support of leaves, flowers, and fruits, the transport of water between the roots and the shoots in xylem and phloem, and the storage of water [1, 2]. In water storage role, stems serve as reservoirs which vary in water content diurnally due to the imbalance between root water uptake and transpiration water loss [3]. And stem water content (StWC) also affects the transport of nutrients and the storage of carbohydrates [4]. Moreover, a better understanding of stem water content contributes to solving some research hotspots in forestry including drought resistance [5], cold resistance [6], precise irrigation [7], and health assessment [8]. Hence, it is significant to study how to measure stem water content. So far, the detecting methods of stem water content can be roughly divided into three categories according to

measuring principles, that is, the oven-drying method, image analysis method, and electronic transducer method.

The oven-drying method is a traditional way to estimate the water content in the stem. By measuring the weight difference between the original wet stem and the stem dried by an oven, the stem water content can be directly calculated. Compared with other detecting methods, the oven-drying method is the most accurate, but it is a destructive measurement. Hence, this method is usually used for calibrating and evaluating other detecting methods. In order to achieve the purpose of nondestructive measurement, some researchers began using various image analysis methods to detect stem water content. According to the imaging principles, the image analysis method includes gamma ray densitometry [9], X-ray computer tomography [10], and nuclear magnetic resonance imaging (MRI) [11]. The density map of water in the stem can be selected as an index to estimate the stem water content. By using a gamma ray densitometer or X-ray

computer tomograph, the density map of water in the stem can be acquired [9, 10]. Combined with the prior calibration model of various types of stem specimens, the stem water content can be calculated. Although both methods are highly sensitive, accurate, and nondestructive, safety concerns of radiation exposure have greatly restricted the further application of the methods [12]. For ensuring the safety of the operator, a secure imaging method called MRI can be an alternative solution for detecting stem water content. By utilizing an MRI system, the density map of water in the stem can be obtained [11]. Based on different image processing algorithms, the stem water content can be computed under different precisions. However, all the methods cannot realize in situ and real-time monitoring of stem water content.

With the development of the electronic detection technology, diverse electronic transducer methods have been applied to detect StWC in situ and in real time, including stem diameter transduction [13–15], time-domain reflection (TDR) [16–19], and frequency-domain (FD) [20–22] capacitance. Many researches have showed that the diurnal variation of StWC appears as a single peak curve with stem tissue absorbing and losing water, causing changes in stem diameter. Hence, the StWC can be estimated by measuring stem diameter variation (SDV) with some high-precision displacement sensors. Fernández and Cuevas [15] adopted LVDT sensors to measure SDV which can be automatically and continuously recorded, suggesting that SDV outputs were influenced by various factors, such as plant age and size, seasonal growth patterns, and sensor position on the stem, apart from StWC. Therefore, the interpretation of SDV data is extremely complex and difficult, which also limits their availability for measuring the StWC. In the meantime, some researchers began studying how to estimate StWC by detecting the apparent dielectric constant of the plant stem. Wullschleger et al. [17] used the TDR method to measure the apparent dielectric constant of stem and then calculate the StWC, indicating that there was a high consistency between the apparent dielectric constant and the StWC. The results turned out that the StWC measured by the TDR method broadly accorded with the oven-drying method, but the probes of sensor were required to insert into the stem, resulting in tissue injury in the stem. In order to reduce the damage caused by probes, some researchers began to investigate the effect of probe length on sensor performance [18, 19]. Experiments have demonstrated that the shorter probes can reduce the damage of stem tissue and the measurement error caused by the difference of water distribution in the stem, but the resolution of the sensor also decreases. And the longer probes increase the signal attenuation, resulting in the larger measurement error. The FD method measures the StWC by taking advantage of the dielectric property of stem as well as the TDR method, but it is noninvasive. Holbrook et al. [20] used FD sensor working at 40 kHz to observe the StWC of palm trees, revealing that the sensor outputs were affected by dielectric loss caused by the ion concentration in stem water. Previous researches have showed that the dielectric loss was largely determined by measurement frequency and the optimal measurement frequency was 100 MHz minimizing the dielectric loss [23].

Considering the defects of the above methods, there are few noninvasive, in situ, real-time, safe, and low-cost methods for detecting the stem water content of woody plants. In the meantime, previous studies suggest that the sensor based on standing wave ratio has a good performance for measuring forest duff water content, but it is not available for the nondestructive measurement of stem water content on account of its long probes [24]. Therefore, the authors decided to design a novel sensor called as StWC sensor for detecting stem water content noninvasively in situ and in real time based on the measuring principle of standing wave ratio. Moreover, extensive experiments were conducted to analyze the performance of the sensor, demonstrating that the sensor has sufficient sensitivity to detect the stem water content of woody plants.

## 2. Materials and Methods

*2.1. Measuring Principle of the Standing Wave Ratio.* The plant stem is mainly composed of wood and water. At a certain measurement frequency, the dielectric constant of water is about 81 which is much larger than that of wood with the dielectric constant of 3. So, the apparent dielectric constant of the plant stem is greatly dominated by the StWC. Hence, the StWC can be estimated by measuring the apparent dielectric constant of the plant stem. In the field of radio frequency, standing wave ratio (SWR) is a measure of the load impedance relative to the characteristic impedance of a transmission line or waveguide [25, 26]. Based on the load impedance, the apparent dielectric constant of measured object can be calculated.

Based on the SWR method, the StWC sensor was designed and manufactured. As illustrated in Figure 1, the StWC sensor mainly consists of a 100 MHz oscillator, a 50  $\Omega$  coaxial transmission line, two wave detectors, an amplifier, and a pair of ring probes. Initially, the high-frequency electromagnetic wave generated by the oscillator spreads along the transmission line. Due to impedance mismatching between the transmission line and the ring probes wrapping around the plant stem snugly, partial incident wave will be reflected back towards the source. Eventually, the incident wave and the reflected wave form a stable standing wave in the transmission line. Hence, the StWC sensor output  $\Delta U$  can be computed as follows:

$$\Delta U = \beta(U_a - U_b) = 2\beta A\rho = 2\beta A \frac{(Z_l - Z_0)}{(Z_l + Z_0)}, \quad (1)$$

where  $\beta$  is the amplification factor of the amplifier;  $U_a$  and  $U_b$  are the voltages at the both ends of the transmission line measured by wave detectors;  $A$  is the amplitude of the oscillator;  $\rho$  is called reflection coefficient;  $Z_0$  is the impedance of the transmission line;  $Z_l$  is the probe detection impedance. Among all the parameters, only  $Z_l$  is undetermined. Hence, it is necessary to further analyze the detection impedance model of the ring probe.

The impedance characteristics of the ring probe are related to the dielectric constant of the material filled in it.

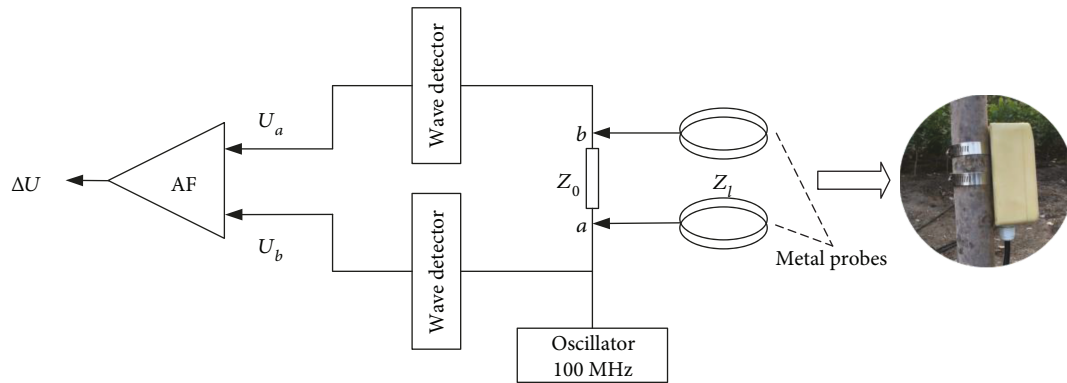


FIGURE 1: Schematic diagram of the StWC sensor.

The capacitance value of ring probe  $C$  is described as follows:

$$C = g\varepsilon_r\varepsilon_0, \quad (2)$$

where  $g$  is a constant related to the diameter of ring probe;  $\varepsilon_r$  is the dielectric constant of medium filled in ring probe;  $\varepsilon_0$  is the dielectric constant in vacuum.

If taking the structure in Figure 2 as the detection impedance model of the ring probe, the expression of its characterization capacitance is shown as follows:

$$C_s = C_t + C^*, \quad (3)$$

where  $C_s$  is the characterization capacitance of ring probe;  $C_t$  is the spurious capacitance generated by electric field;  $C^*$  is the characterization capacitance of measured stem.

It can be concluded from equation (2) that  $C^*$  can be calculated by  $C^* = g_m\varepsilon_{r,m}\varepsilon_0$ , where subscript  $m$  denotes the medium. Admittance  $Y$  and detection impedance  $Z_l$  of ring probe are expressed as follows:

$$Y = \frac{1}{Z_l} = j\omega C_s = j\omega C_t + j\omega C^*, \quad (4)$$

where  $\omega$  is the angular frequency of the oscillator.

In the detection process, the electric conductivity of the stem will have an effect on the impedance of the probe as follows:

$$j\omega C^* = j\omega g_m\varepsilon_{r,m}\varepsilon_0 + G, \quad (5)$$

where  $G$  is the impedance produced by ionic conductivity of solution in the stem.

Among all the parameters of the probe detection impedance,  $C_t$ ,  $\omega$ , and  $\varepsilon_0$  are determined.  $g_m$ ,  $\varepsilon_{r,m}$ , and  $G$  are undetermined and related with measured stem. In the meanwhile,  $\varepsilon_{r,m}$  and  $G$  are also affected by stem temperature. In conclusion, the sensor output is determined by stem diameter, dielectric constant, electric conductivity, and temperature. Among these four factors, stem dielectric constant is the measured object. In order to accurately measure stem dielectric constant, the effects of stem diameter, electric conductivity, and temperature on sensor output must be calibrated.

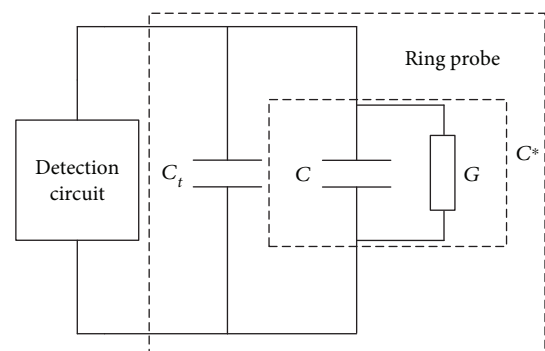


FIGURE 2: Circuit model of ring probe detection impedance.

**2.2. Components of StWC Sensor.** Following the proof of concept presented in the previous section, a noninvasive sensor was manufactured to allow the in situ measurement of stem water content. The various components of StWC sensor are presented in Figure 3. The printed circuit board (PCB) was designed according to the schematic diagram presented in Figure 1. The ring probe is made of ASTM 304 stainless steel applicable to field environment. And its diameter can be adjusted to adapt to the plant stems with different sizes ranging from 21 to 95 mm by the rotary knob. The screw bolt is a connector between ring probe and probe port. The body case is made of white resin with a lower dielectric constant. And the mounting holes are used to fix the PCB and ring probes.

**2.3. Physical Model of Ring Probe and Surrounding Medium.** The StWC sensor has two ring probes which were designed as an upper and a lower ring with a spacing of 17.6 mm. In the absence of a specific statement, the diameter of the ring was set as 55 mm. As illustrated in Figure 4, a physical model of ring probe and surrounding medium was established by using electromagnetic field simulation software, namely, HFSS. The solution frequency was set as 100 MHz and the excitation was set as lumped port. Medium inside the ring probe was set as water and its dielectric constant is 81. Medium outside the ring probe was set as air and its dielectric constant is 1. The ring probe was set as an ideal electric field boundary, and a cylinder with a diameter of 70 mm and a

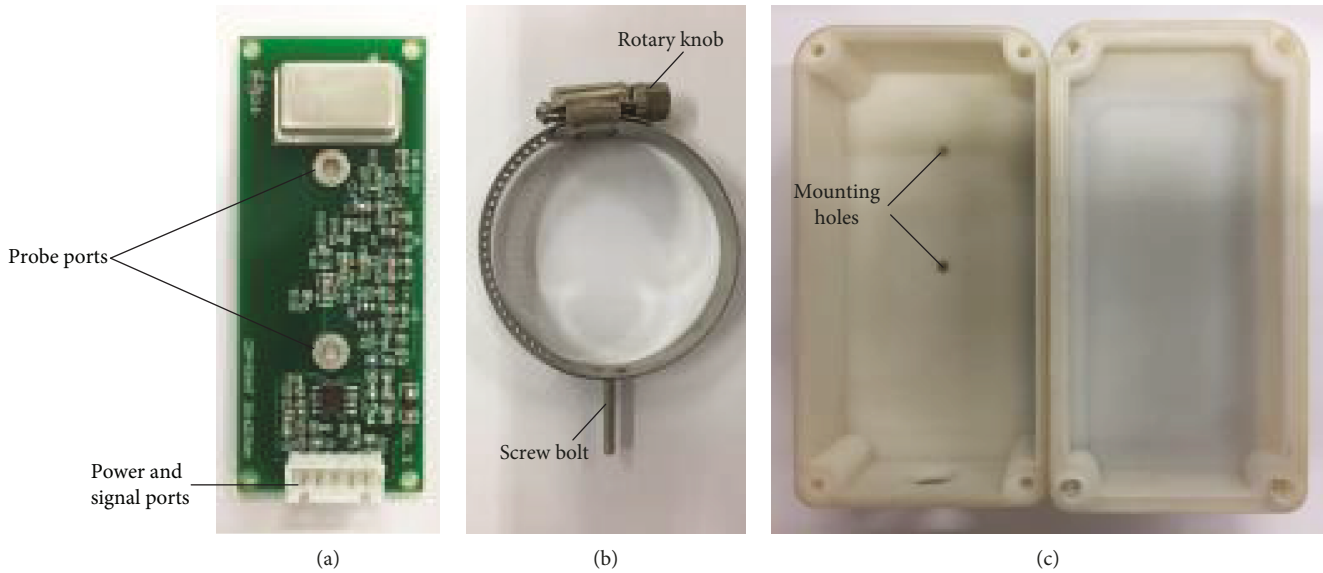


FIGURE 3: Components of StWC sensor: (a) printed circuit board (width: 30 mm, height: 74 mm); (b) ring probe (width: 12.6 mm, thickness: 0.65 mm); (c) body case (width: 56 mm, height: 100 mm, and depth: 48 mm).

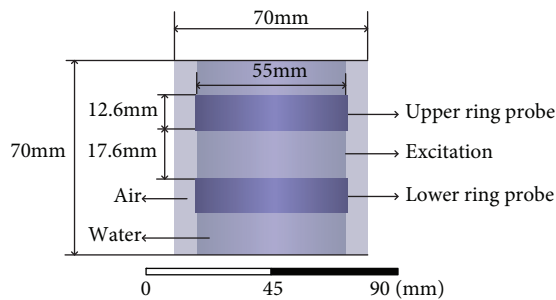


FIGURE 4: Physical model of ring probe and surrounding medium.

height of 70 mm was used as the radiation boundary condition. Ultimately, the physical model was used to test the sensitive distance of StWC sensor.

**2.4. Experimental Design and Procedure.** The organic glass beaker with known diameter was chosen to simulate plant bark. The solution with known dielectric constant was chosen to simulate the stem water content. Therefore, the beaker filled with solution can be regarded as a simulated plant stem which was acted as the experimental object in following experiments. Then the experiments were divided into four parts: determining the sensitive distance of the sensor in axial and radial direction, calibrating the effects of dielectric constant, electric conductivity, temperature, and stem diameter on the sensor, analyzing the performance of the sensor in practical application, and comparing the performance between StWC sensor and Testo 606-2 (Testo, Germany; range: <60%, accuracy:  $\pm 1\%$ ). In this study, the sensor sensitivity indicates how much the sensor's output changes when the input quantity being measured changes.

In the first part, the beaker with a diameter of 55 mm was selected as the experimental object. The sensitive distance of

the sensor in axial direction was determined by changing the water surface height from 0 to 80 mm in the beaker. The sensitive distance of the sensor in radial direction was determined by changing the sealed glass tube which was placed in the center of the water-filled beaker and displaced water near the center. The diameter of the sealed glass tube ranged from 0 to 52 mm. In the second part, the beaker was filled with different solutions in different experiments. As can be seen from Table 1, solutions with known dielectric constant from 6 to 81 were formulated from a mix of ethyl acetate, isoamylol, n-butanol, isopropanol, ethanol, glycol, and water. As shown in Table 2, solutions with known electric conductivity from 0.53 to  $16 \text{ mS}\cdot\text{cm}^{-1}$  were formulated from a mix of water and salt. Solutions with known temperature from 0 to  $60^\circ\text{C}$  were formulated from a mix of cold and hot water. The effects of dielectric constant, electric conductivity, and temperature on the sensor were calibrated by using the abovementioned solutions in the beaker with a diameter of 55 mm. The effect of stem diameter on the sensor was calibrated by changing the beaker from 20 to 55 mm in diameter. In the third part, the crape myrtle with a diameter of 42 mm was selected as the experimental object. The tree was transplanted into a pot where soil moisture content was approximately 25% and the soil surface was covered by plastic wrap to prevent water from evaporating. The weight of the pot was monitored synchronously to calculate the whole-tree transpiration. In the meantime, the StWC of the crape myrtle was continuously monitored by StWC sensor. The stem temperature was measured by customized platinum electrode with 1 mm in diameter and 20 mm in length which can drastically reduce the damages to the stem. The platinum electrode was inserted into the stem in radial direction and penetrated through the xylem. Both StWC sensor and platinum electrode were installed at breast height. This experiment was conducted in a greenhouse where a micro weather station was installed for acquiring environmental

TABLE 1: Formula of solutions with different dielectric constants (DCs).

Parameter	Ethyl acetate	Isoamylol	n-Butanol	Isopropanol	Ethanol	Glycol	Ethanol : water (1 : 1) <sup>1</sup>	Ethanol : water (1 : 2)	Water
DC	6.0	15.2	17.5	19.9	24.6	37.7	52.8	62.2	81.0

<sup>1</sup>The ratio was calculated by volume.

TABLE 2: Formula of solutions with different electric conductivities (ECs).

Parameter	Value									
Water content (kg)	1	1	1	1	1	1	1	1	1	1
Salt content (g) <sup>1</sup>	0.00	1.00	2.08	3.20	4.32	5.44	6.61	7.82	9.03	10.25
EC (mS·cm <sup>-1</sup> )	0.53	2.44	4.32	6.15	7.72	8.64	10.37	12.3	13.45	16.00

<sup>1</sup>The content of NaCl is more than 99.1%.

parameters including stem temperature, air temperature, air humidity, and photosynthetically active radiation (PAR) on May 1, 2018. The diurnal average, minimum value, and maximum value of air temperature were 22.7, 17.7, and 32.1°C, respectively. The diurnal average, minimum value, and maximum value of air humidity were 48, 26, and 72%, respectively. The diurnal average, minimum value, and maximum value of PAR were 230, 33, and 991  $\mu\text{mol}\cdot\text{m}^{-2}\cdot\text{s}^{-1}$ , respectively. In the last part, the monitored crape myrtle was cut into several stem segments with a length of 65 mm. During the oven-drying process of the stem segment, we recorded StWC sensor outputs and the weights of the stem segment simultaneously which were used to calibrate the sensor. Meanwhile, the moisture of stem segment was measured by Testo 606-2. In all experiments, the sensor was installed on the beaker or stem and its outputs were automatically recorded by the self-developed data logger.

### 3. Results and Discussion

**3.1. Sensitivity Determination.** By establishing the physical model of ring probe and surrounding medium in HFSS, the electric field distribution of ring probe in axial and radial direction was simulated (Figure 5). It can be seen that the electric field intensity outside the ring probe is considerably larger than that inside the ring probe, indicating that the attenuation of internal electric field is faster than that of external electric field at the same distance. The result is consistent with the fact that the attenuation of electric field in medium has a positive correlation with the dielectric constant of the medium. Hence, the internal electric field of ring probe can be used to detect stem water content. Figure 5 also shows that the sensor is the most sensitive to water in the process of internal electric field decreasing by 74% (from 121 to 31  $\text{V}\cdot\text{m}^{-1}$  in axial direction and from 31 to 8  $\text{V}\cdot\text{m}^{-1}$  in radial direction). On these grounds, the conclusion can be drawn that the sensitive distance of the sensor is approximately 52 mm in axial direction and 18.5 mm in radial direction.

The rule that sensor output changes with the height of water surface as it moves through the two ring probes is shown in Figure 6(a). The axial sensitivity of the sensor is the slope of the curve which shows an obvious S-shaped

pattern, indicating that the axial sensitivity gradually increases as the water moves through the lower ring, reaches a maximum as the water is in the middle of two rings, and then gradually decreases as the water moves through the upper ring. As a whole, the axial sensitive distance of the sensor is approximately 53 mm (the distance between the two red points in Figure 6(a)). The rule that sensor output changes with the diameter of sealed glass tube as it excludes the water from the center of the beaker to the edge is shown Figure 6(b). The slope of the curve gradually increases as the diameter of sealed glass tube increases, indicating that the radial sensitivity of the sensor has a negative correlation with the radial distance between the ring probe and the medium. Overall, the radial sensitive distance of the sensor is approximately 20 mm (the half distance between the two red points in Figure 6(b)). Comparing Figures 5 and 6, it can be concluded that there is a high consistency concerning the sensitive distance of the sensor in both simulation experiments and validation experiments.

**3.2. Dielectric Constant, Electric Conductivity, Temperature, and Stem Diameter Calibration.** Figure 7(a) shows the responses of the sensor output to solutions with relative dielectric constant from 6 to 81 which is approximately equivalent to StWC from 0.01 to 1.00  $\text{cm}^3\cdot\text{cm}^{-3}$  [17]. And the trend line of the data shows a linear relation between sensor output and relative dielectric constant with determination coefficient equal to 0.9677, indicating that the sensor can detect stem water content in a full range covering all woody plants. The stem tissue fluid has a certain value of electric conductivity caused by various solutes and changing with StWC. The effect of electric conductivity on the sensor output is shown in Figure 7(b). Comparing Figures 7(a) and 7(b), it can be concluded that the sensor sensitivity to electric conductivity (28.4 mV (mS·cm<sup>-1</sup>)<sup>-1</sup>) is larger than that to dielectric constant (9.2 mV), indicating that the impact of electric conductivity on the sensor cannot be ignored. The effect of temperature change on the sensor output is mainly embodied in two aspects including the impacts of temperature on dielectric constant and electric conductivity. According to previous researches, the temperature coefficient of dielectric constant is negative [27, 28] and the temperature coefficient of electric conductivity is positive

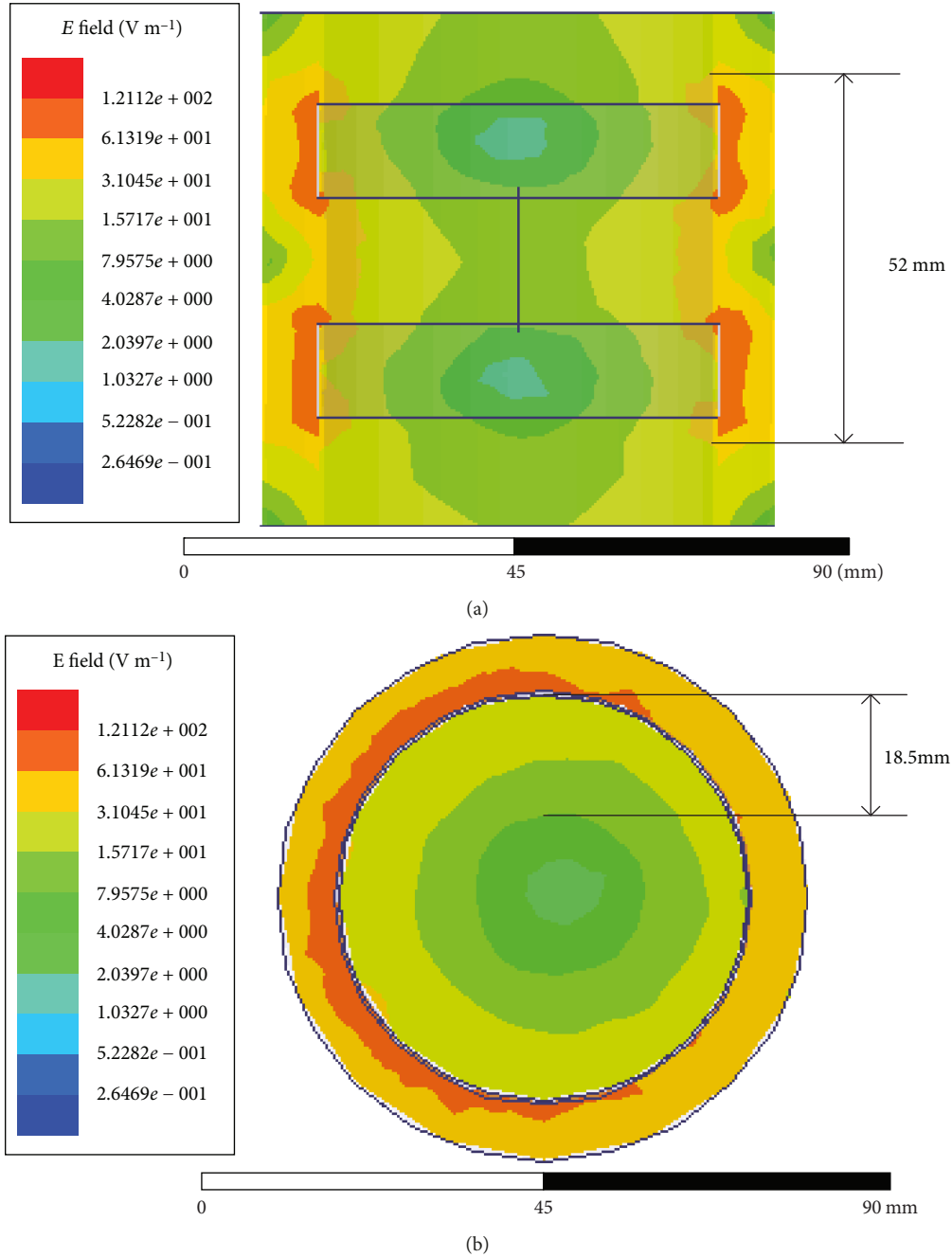


FIGURE 5: (a) Simulation of electric field distribution of ring probe in axial direction. (b) Simulation of electric field distribution of ring probe in radial direction.

[29]. As can be seen from Figure 7(c), the sensor sensitivity to temperature is negative ( $-1.0 \text{ mV}^\circ\text{C}^{-1}$ ), revealing that the sensor output is greatly dominated by the temperature coefficient of dielectric constant in the experiment. Considering the growth of stem diameter, it is necessary to analyze the relation between stem diameter and sensor output. As shown in Figure 7(d), the sensor output is sensitive to stem diameter ( $22.1 \text{ mV mm}^{-1}$ ), confirming that the probe detection impedance is influenced by the diameter of ring probe which has been mentioned in measuring principle. Combined with the radial sensitive distance of the sensor, the conclusion can be

drawn that the maximum stem diameter in which the sensor can be used to measure the StWC accurately is approximately 40 mm. In the meanwhile, considering that water transport and storage are greatly dominated by the xylem, therefore when the stem diameter is slightly larger than 40 mm but the distance between the inner edge of the xylem and the outer edge of the bark is less than 20 mm, the sensor is still able to measure the StWC with certain accuracy.

*3.3. Performance Analysis of StWC Sensor in Practical Application.* In order to detect the StWC of a certain tree

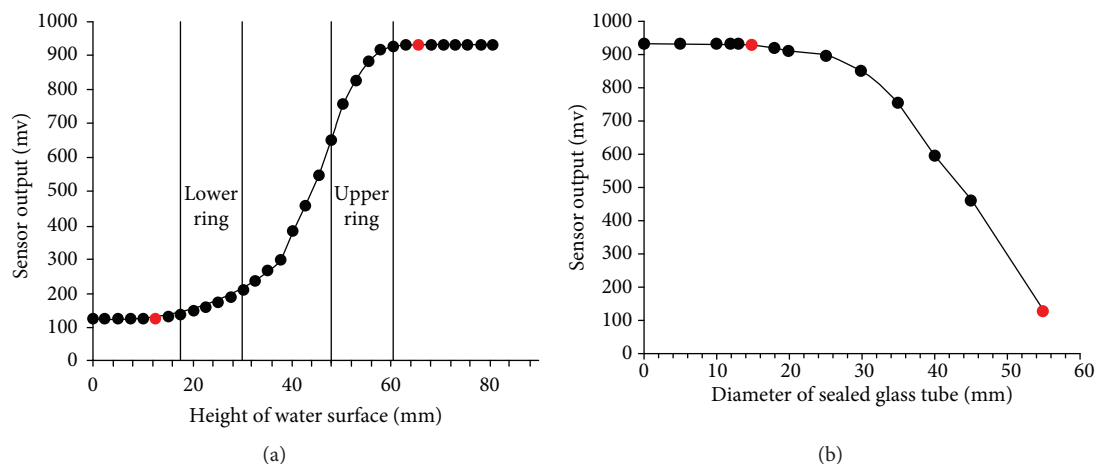


FIGURE 6: (a) Sensitivity of StWC sensor in axial direction. (b) Sensitivity of StWC sensor in radial direction.

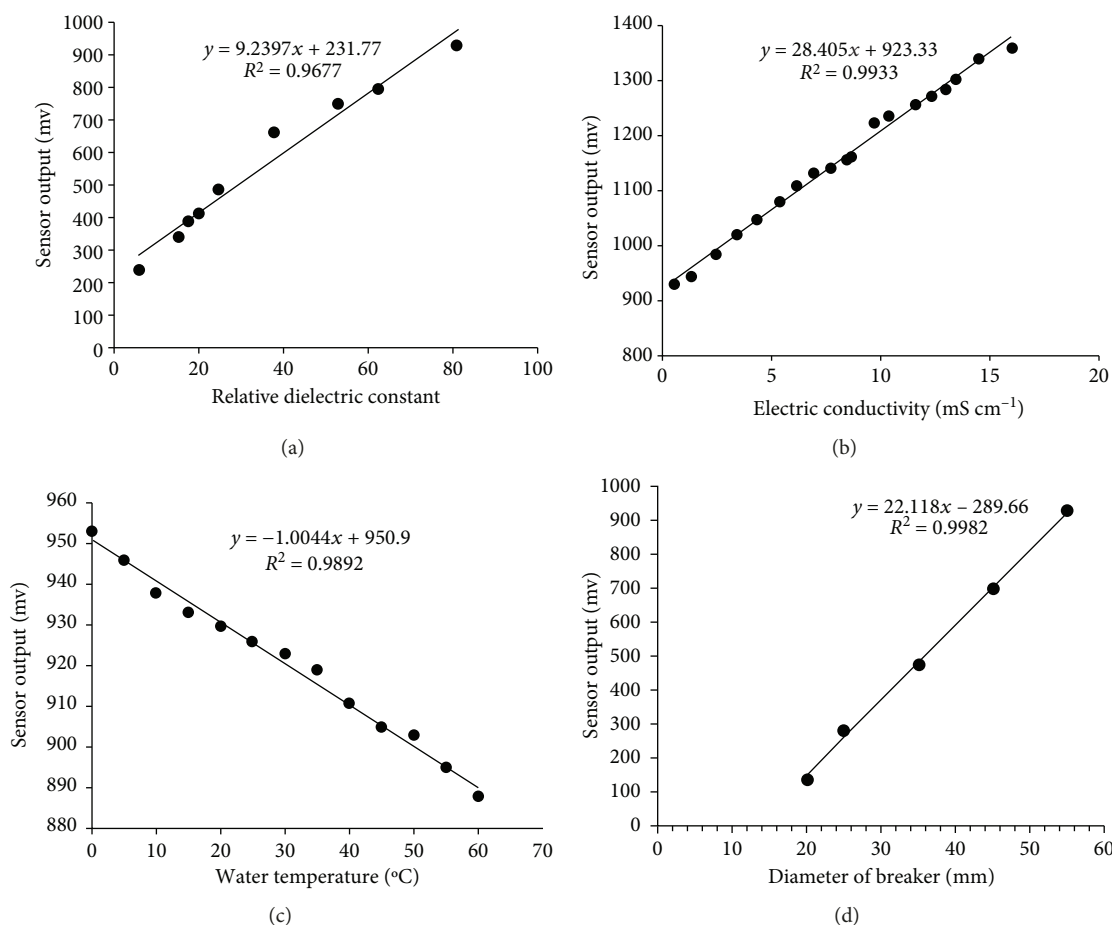


FIGURE 7: (a) The effect of dielectric constant on StWC sensor. (b) The effect of electric conductivity on StWC sensor. (c) The effect of temperature on StWC sensor. (d) The effect of stem diameter on StWC sensor.

species accurately, it is essential to use the real stem segment to calibrate the sensor with the oven-drying method. During the oven-drying process of the stem segment, the mixed dielectric constant of water and wood gradually decreases with the evaporation of water, thus resulting in the decrease

of sensor output. According to Figure 8(a), there is a linear relation between the StWC of the crape myrtle and the sensor output with the high sensitivity equal to  $1022.1 \text{ mV} (\text{cm}^3 \text{ cm}^{-3})^{-1}$ , indicating that the sensor is able to measure the StWC precisely. Then the correction parameters were

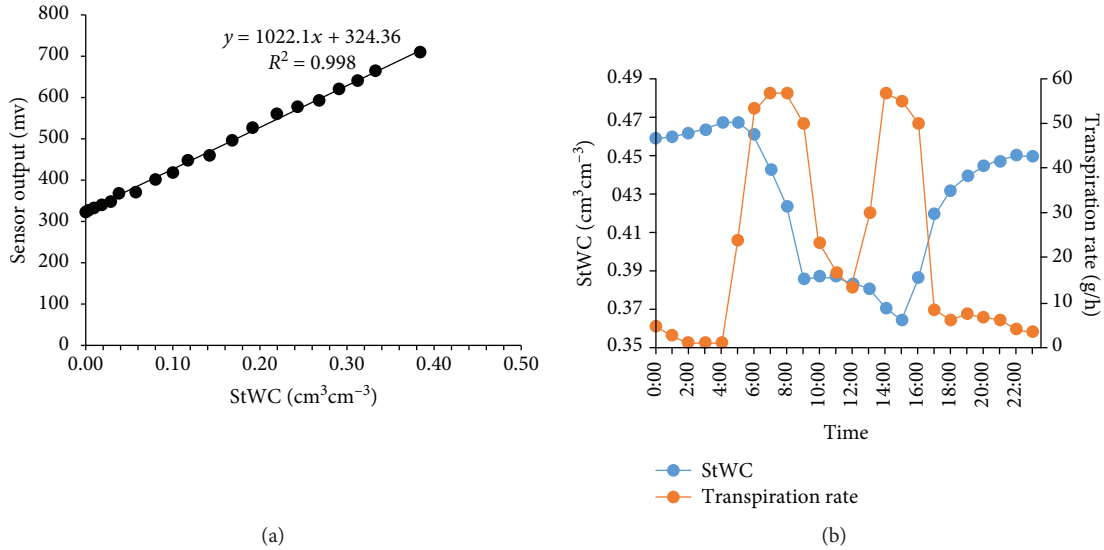


FIGURE 8: (a) Calibration curve of StWC sensor obtained from the stem segment oven-drying method. (b) The diurnal StWC of the crape myrtle in response to the transpiration rate.

used to calculate StWC in Figure 8(b) which shows the diurnal StWC of the crape myrtle in response to the transpiration rate estimated from the weighting experiment. As the transpiration rate increases in the morning, water loss rate by leaf transpiration is greater than water absorption rate by root, thus resulting in the fast fall of StWC. Nevertheless, when the transpiration rate reaches a certain threshold at midday, there is a dynamic balance between water loss and water absorption due to the midday depression, thus causing the small fluctuations of StWC. As the transpiration rate decreases at nightfall, water loss rate by leaf transpiration is smaller than water absorption rate by root, thus resulting in the fast rise of StWC. Moreover, when the transpiration rate is very weak at night, the roots continue to absorb water by root pressure, thus causing the slow rise of StWC. From an overall perspective, the diurnal fluctuation of StWC was approximately 10.3% which was equal to the diurnal change of sensor output of 105.28 mV from morning to midday. We presumed that the mass of salt was a constant and the average EC was  $10 \text{ mS}\cdot\text{cm}^{-1}$  in stem tissue fluid [30]. Therefore, the 10.3% StWC change yielded an EC change of 10.3% equal to  $1.03 \text{ mS}\cdot\text{cm}^{-1}$  which corresponded to a signal change of 29.26 mV. In the meanwhile, the diurnal fluctuation of stem temperature was  $14.5^\circ\text{C}$  which caused a signal response of -14.56 mV. Because of the opposite impacts of EC and temperature on sensor output, the correction to sensor output might be 14.70 mV which was about 14.0% of the diurnal change of sensor output. In addition, a 12-bit A/D converter with the reference voltage of 2.5 V was used in the data logger, causing a voltage uncertainty of  $\pm 0.61 \text{ mV}$  which can be ignored compared with the effects of stem EC and temperature. Hence, the combined effects of stem EC and temperature on sensor output are significant and it is necessary to correct the error caused by the two factors.

3.4. Comparing the Performance between StWC Sensor and Testo 606-2. After StWC sensor was calibrated by drying some stem segments, the performance of both StWC sensor and Testo 606-2 was tested by drying the remaining stem segments. It can be assumed that StWC measured by the oven-drying method was a true value. As shown in Figure 9, the values measured by StWC sensor is closer to the true value than that measured by Testo 606-2. In addition, when the true value is larger than 2%, the values measured by Testo 606-2 are significantly smaller than the true value. This is because the probe length of Testo 606-2 is less than 10 mm, limiting its measuring depth to the superficial layer. During the oven-drying process of the stem segment, the water evaporation of superficial layer was faster than that of deep layer, causing a lower value measured by Testo 606-2. Although its measuring depth can be improved by increasing probe length, the longer probe may destroy the structure of the plant stem, causing the difference in water distribution. In the meanwhile, the measuring errors of two sensors were calculated to evaluate measuring accuracy (Table 3). Compared with the true value, the errors (maximum error, average error, and RMSE) of StWC sensor are obviously smaller than those of Testo 606-2. Hence, the conclusion can be drawn that the measuring accuracy of StWC sensor is higher than that of Testo 606-2 for detecting stem water content.

## 4. Conclusions

In this paper, we designed a novel sensor for detecting stem water content noninvasively based on the measuring principle of standing wave ratio. In addition, extensive experiments were carried out to analyze the performance of the sensor. The main conclusions are as follows:

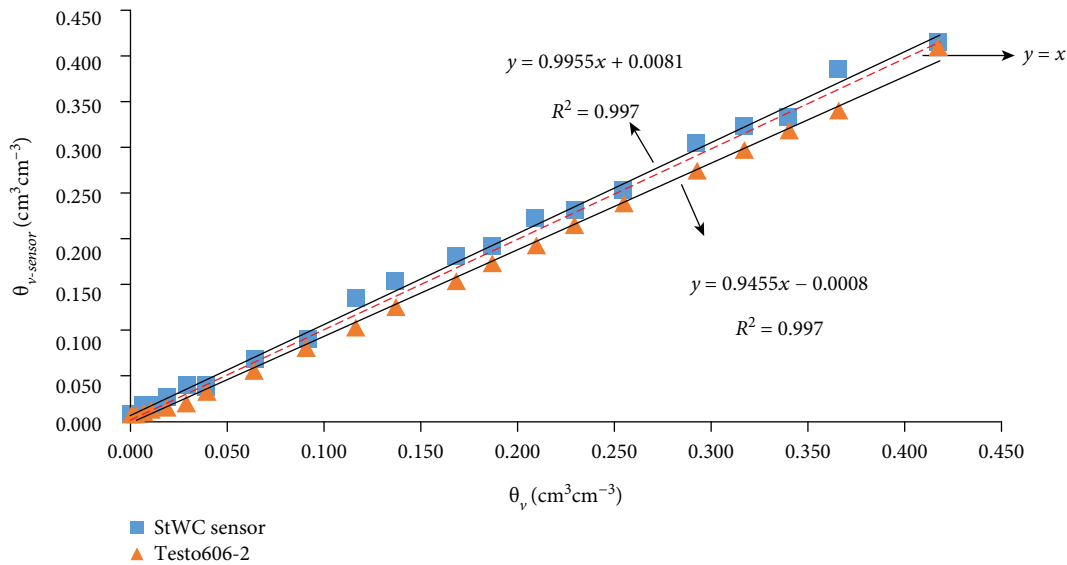


FIGURE 9: StWC measured by the oven-drying method ( $\theta_v$ ) vs. StWC measured by StWC sensor and Testo 606-2 ( $\theta_{V\text{-sensor}}$ ).

TABLE 3: Error analysis of StWC measurements using StWC sensor and Testo 606-2.

Sensor type	Maximum error ( $\text{cm}^3 \text{cm}^{-3}$ )	Average error ( $\text{cm}^3 \text{cm}^{-3}$ )	RMSE ( $\text{cm}^3 \text{cm}^{-3}$ )
StWC sensor	0.020	0.008	0.010
Testo 606-2	0.025	0.012	0.013

First, the apparent dielectric constant of the plant stem is greatly determined by the stem water content. There is a good linear relation between the signal output of StWC sensor and the dielectric constant of measured object with measuring range of StWC from 0.01 to 1.00  $\text{cm}^3 \text{cm}^{-3}$ , indicating that the sensor can detect stem water content in a full range covering all woody plants.

Second, because the water in the plant stem can weaken the internal electric field of StWC sensor greatly, the sensitive distance of the sensor is limited. Generally speaking, the sensitive distance of the sensor is approximately 53 mm in axial direction and 20 mm in radial direction, revealing that the maximum stem diameter in which the sensor can be used to measure the StWC accurately is approximately 40 mm.

Third, the sensor sensitivity to electric conductivity is positive and the sensor sensitivity to temperature is negative. However, the combined effects of stem EC and temperature on sensor output are significant and it is necessary to correct the error caused by the two factors. Moreover, there is a good linear relation between the signal output of StWC sensor and stem diameter with high sensitivity of  $22.1 \text{ mV mm}^{-1}$ , demonstrating that it is essential to calibrate the sensor according to the diameter of the plant stem.

Finally, compared with the oven-drying method, StWC sensor has higher measuring accuracy than Testo 606-2 and its average error is less than  $0.01 \text{ cm}^3 \text{cm}^{-3}$ . In addition, the sensor performed very well on the crape myrtle with high

sensitivity equal to  $1022.1 \text{ mV} (\text{cm}^3 \text{cm}^{-3})^{-1}$ , indicating that the sensor is able to measure the StWC precisely in practice.

## Data Availability

The data used to support the findings of this study are available from the corresponding author upon request.

## Conflicts of Interest

The authors declare no conflict of interest.

## Authors' Contributions

For this research article, Chao Gao and Yandong Zhao conceived and designed the experiments; Chao Gao performed the experiments; Chao Gao and Yue Zhao analyzed the data; Chao Gao, Yue Zhao, and Yandong Zhao wrote the paper.

## Acknowledgments

This research was funded by the National Key Research and Development Program of China (Grant No. 2017YFD0600901), the Beijing Municipal Science and Technology Commission (Grant No. Z161100000916012), and the Special Fund for Beijing Common Construction Project.

## References

- [1] M. T. Tyree and F. W. Ewers, "The hydraulic architecture of trees and other woody plants," *New Phytologist*, vol. 119, no. 3, pp. 345–360, 1991.
- [2] T. W. J. Scheenen, F. J. Vergeldt, A. M. Heemskerk, and H. Van As, "Intact plant magnetic resonance imaging to study dynamics in long-distance sap flow and flow-conducting surface area," *Plant Physiology*, vol. 144, no. 2, pp. 1157–1165, 2007.

- [3] S. Dzikiti, K. Steppe, R. Lemeur, and J. R. Milford, "Whole-tree level water balance and its implications on stomatal oscillations in orange trees [*Citrus sinensis* (L.) Osbeck] under natural climatic conditions," *Journal of Experimental Botany*, vol. 58, no. 7, pp. 1893–1901, 2007.
- [4] P. E. H. Minchin and A. Lacombe, "New understanding on phloem physiology and possible consequences for modelling long-distance carbon transport," *New Phytologist*, vol. 166, no. 3, pp. 771–779, 2005.
- [5] M. Farooq, A. Wahid, N. Kobayashi, D. Fujita, and S. M. A. Basra, "Plant drought stress: effects, mechanisms and management," *Agronomy for Sustainable Development*, vol. 29, no. 1, pp. 185–212, 2009.
- [6] P. E. Verslues, M. Agarwal, S. Katiyar-Agarwal, J. Zhu, and J. K. Zhu, "Methods and concepts in quantifying resistance to drought, salt and freezing, abiotic stresses that affect plant water status," *Plant Journal*, vol. 45, no. 4, pp. 523–539, 2006.
- [7] A. Patakas, B. Noitsakis, and A. Chouzouri, "Optimization of irrigation water use in grapevines using the relationship between transpiration and plant water status," *Agriculture Ecosystems and Environment*, vol. 106, no. 2-3, pp. 253–259, 2005.
- [8] R. A. Spotts, "Photosynthesis, transpiration, and water potential of apple leaves infected by *Venturia inaequalis*," *Phytopathology*, vol. 69, no. 7, pp. 717–719, 1979.
- [9] W. R. N. Edwards and P. G. Jarvis, "A method for measuring radial differences in water content of intact tree stems by attenuation of gamma radiation," *Plant, Cell and Environment*, vol. 6, no. 3, pp. 255–260, 1983.
- [10] A. Raschi, R. Tognetti, H. W. Ridder, and C. Beres, "Water in the stems of sessile oak (*Quercus petraea*) assessed by computer tomography with concurrent measurements of sap velocity and ultrasound emission," *Plant, Cell and Environment*, vol. 18, no. 5, pp. 545–554, 1995.
- [11] V. De Schepper, D. van Dusschoten, P. Copini, S. Jahnke, and K. Steppe, "MRI links stem water content to stem diameter variations in transpiring trees," *Journal of Experimental Botany*, vol. 63, no. 7, pp. 2645–2653, 2012.
- [12] H. G. Jones, "Irrigation scheduling: advantages and pitfalls of plant-based methods," *Journal of Experimental Botany*, vol. 55, no. 407, pp. 2427–2436, 2004.
- [13] T. Simonneau, R. Habib, J. P. Goutouly, and J. G. Huguet, "Diurnal changes in stem diameter depend upon variations in water content: direct evidence in peach trees," *Journal of Experimental Botany*, vol. 44, no. 3, pp. 615–621, 1993.
- [14] R. Zweifel, H. Item, and R. Häsler, "Stem radius changes and their relation to stored water in stems of young Norway spruce trees," *Trees*, vol. 15, no. 1, pp. 50–57, 2000.
- [15] J. E. Fernández and M. V. Cuevas, "Irrigation scheduling from stem diameter variations: a review," *Agricultural and Forest Meteorology*, vol. 150, no. 2, pp. 135–151, 2010.
- [16] A. Nadler, E. Raveh, U. Yermiyahu, and S. R. Green, "Evaluation of TDR use to monitor water content in stem of lemon trees and soil and their response to water stress," *Soil Science Society of America Journal*, vol. 67, no. 2, pp. 437–448, 2003.
- [17] S. D. Wullschleger, P. J. Hanson, and D. E. Todd, "Measuring stem water content in four deciduous hardwoods with a time-domain reflectometer," *Tree Physiology*, vol. 16, no. 10, pp. 809–815, 1996.
- [18] M. Persson and S. Haridy, "Estimating water content from electrical conductivity measurements with short time-domain reflectometry probes," *Soil Science Society of America Journal*, vol. 67, no. 2, pp. 478–482, 2003.
- [19] J. Irvine and J. Grace, "Non-destructive measurement of stem water content by time domain reflectometry using short probes," *Journal of Experimental Botany*, vol. 48, no. 3, pp. 813–818, 1997.
- [20] N. M. Holbrook, M. J. Burns, and T. R. Sinclair, "Frequency and time-domain dielectric measurements of stem water content in the arborescent palm, *Sabal palmetto*," *Journal of Experimental Botany*, vol. 43, no. 1, pp. 111–119, 1992.
- [21] M. Stacheder, F. Koeniger, and R. Schuhmann, "New dielectric sensors and sensing techniques for soil and snow moisture measurements," *Sensors*, vol. 9, no. 4, pp. 2951–2967, 2009.
- [22] W. Skierucha and A. Wilczek, "A FDR sensor for measuring complex soil dielectric permittivity in the 10–500 MHz frequency range," *Sensors*, vol. 10, no. 4, pp. 3314–3329, 2010.
- [23] G. J. Gaskin and J. D. Miller, "Measurement of soil water content using a simplified impedance measuring technique," *Journal of Agricultural Engineering Research*, vol. 63, no. 2, pp. 153–159, 1996.
- [24] X. Yan, Y. Zhao, Q. Cheng, X. Zheng, and Y. Zhao, "Determining forest duff water content using a low-cost standing wave ratio sensor," *Sensors*, vol. 18, no. 2, 2018.
- [25] S. B. Cohn, "Optimum design of stepped transmission-line transformers," *IRE Transactions on Microwave Theory and Techniques*, vol. 3, no. 3, pp. 16–20, 1955.
- [26] S. Roberts and A. Von Hippel, "A new method for measuring dielectric constant and loss in the range of centimeter waves," *Journal of Applied Physics*, vol. 17, no. 7, pp. 610–616, 1946.
- [27] E. Lange and A. L. Robinson, "The temperature coefficient of the dielectric constant of water," *Journal of the American Chemical Society*, vol. 52, no. 7, pp. 2811–2813, 1930.
- [28] J. M. Wraith and D. Or, "Temperature effects on soil bulk dielectric permittivity measured by time domain reflectometry: experimental evidence and hypothesis development," *Water Resources Research*, vol. 35, no. 2, pp. 361–369, 1999.
- [29] D. L. Corwin and S. M. Lesch, "Apparent soil electrical conductivity measurements in agriculture," *Computers and Electronics in Agriculture*, vol. 46, no. 1-3, pp. 11–43, 2005.
- [30] A. Nadler, E. Raveh, U. Yermiyahu et al., "Detecting water stress in trees using stem electrical conductivity measurements," *Soil Science Society of America Journal*, vol. 72, no. 4, pp. 1014–1024, 2008.

